SUPERCONDUCTORS, STABILITY IN FORCED FLOW

Forced-flow–cooled conductors are the preferred choice for magnets that must operate in an electromagnetic and mechanically *noisy* environment, when pulsed operation requires minimization of ac losses, or whenever the operating conditions require a reliable and cost-effective design. In this article we review the guidelines that motivated the choice of forced-flow–cooled conductors to obtain an effective and stable superconductor design for large magnets, such as those for fusion, superconducting magnetic energy storage (SMES), particle detectors, or magneto-hydrodynamic (MHD) application. We will discuss the particular features of the stability margin in forced-flow–cooled conductors and the models commonly used to compute it.

SUPERCONDUCTOR STABILITY

Superconductors exhibit zero resistance only within relatively narrow parameters of temperature, magnetic field, and transport current, below the so-called *critical surface.* When brought outside this region by a disturbance (e.g., by energy deposition stemming from a mechanical motion) superconductivity is lost and Joule heating is generated. If not prevented by other mechanisms, the superconductor cascades further from its nominal operating point into an irreversible process leading to the complete loss of superconductivity in the magnet. This process is commonly known as a *quench.* Even if the magnet is properly protected against damage, a magnet quench is an undesirable event in terms of availability and cost. A well-designed magnet will not quench under normal operating conditions. The study of stability pertains to the understanding of the processes and mechanisms whereby a superconductor will remain (or not) within its operating region, thus ensuring magnet operation without quench. This area of study has evolved through many years of experimentation and analysis.

Stekly Criterion for Cryostability

The first superconducting magnets were cooled by immersion in a helium bath. As we will see later, classical stability theory as derived for these bath-cooled magnets does not directly extend to forced-flow conductors. It is nonetheless useful to review here the oldest and simplest stability criterion developed for bath-cooled conductors, the so-called Stekly criterion of *cryostability* (1). In their original development, Stekly and Zar (1) backed a superconducting material with a low-resistance copper shunt. The cross section A_{Cu} of the shunt was such that in the case of a transition of the superconducting material to the normal state, the maximum Joule heating, obtained when the current I was completely displaced from the superconductor to the copper, was smaller than the heat removal capability at the conductor perimeter p_w wetted by the helium. Under this condition the conductor always recovered from a perturbation, irrespective of the size of the disturbance that caused the quench. In brief, the conductor was unconditionally stable. Writing the simple power balance of heating and cooling, they came to the following criterion for cryostability, formulated using the so-called Stekly parameter α:

$$\alpha = \frac{\rho_{\mathrm{Cu}} I^2}{h p_{\mathrm{w}} A_{\mathrm{Cu}} (T_{\mathrm{c}} - T_{\mathrm{op}})} < 1 \qquad (1)$$

where ρ_{Cu} is the stabilizer resistivity, h the heat transfer coefficient between conductor and cooling bath, T_c is the critical temperature, and T_{op} the bath operating temperature.

Stability versus Perturbation Spectrum

Cryostable conductors have an exceptional tolerance to energy inputs. The drawback is that the resulting operating current density is low, and thus coil size and cost are large. The present approach is different, and consists in designing the conductor to be stable against the spectrum of energy disturbances expected in the magnet, instead of requiring the conductor to be stable against disturbances of arbitrary nature and intensity. This implies a comparison of the initial estimate of the energy release mechanisms and magnitude to the so called energy margin ΔE that we define as the maximum energy deposition that the conductor can tolerate while recovering from the superconducting state. Let us take as an example a conductor in which mechanical energy releases dominate. Following Keilin (2,3), we compare schematically in Fig. 1 the stability margin to the disturbances that can potentially drive the conductor normal. As shown there, the stability margin ΔE decreases with increasing current I, while mechanical disturbances, the curves labeled "D," increase with the current. In this case, the conductor is no longer unconditionally stable but it has an upper stability margin, traditionally expressed in mJ/cm^3 of metal in the cable. The disturbance spectrum must be interpreted as the energy released in each event. At increasing current a single event releases an increasing energy because of the proportionality to either the Lorentz forces (I^2) or to the strain energy in the cable (I^4). As the magnet is charged, the two curves approach, until eventually the spectrum of mechanical disturbances (D) equals and surpasses the stability margin (ΔE). At this point the magnet will quench as soon as a perturbation event will take place. The most likely event during magnet charge-up will be the one associated with the largest energy release. Most mechanical energy inputs are associated with irreversible processes such as stick-and-slip motions and cable compaction. Therefore, once this event has taken place, and the associated energy has been released, the energy perturbation spectrum at the following charge-up will be diminished. We illustrate this situation in Fig. 1 by the set of curves D1, D2, Dn that represent the perturbation spectrum at successive charge-ups 1, 2, . . ., n. The intersection of these curves with the energy margin moves towards higher currents, and we see from this elementary example a simple explanation of the phenomenon of *training* that disappointed early builders of superconducting magnets.

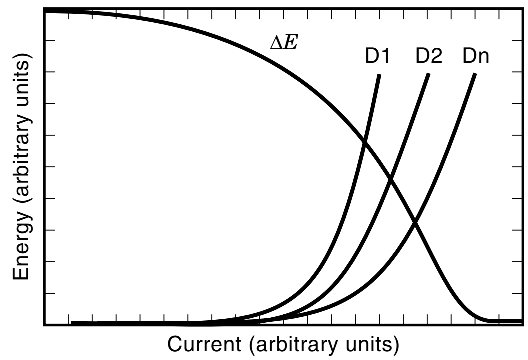

Figure 1. Typical curves for the conductor stability margin (ΔE) and mechanical disturbance spectrum (D).

We see from this simple example that we have two possibilities to guarantee the stable performance of the conductor. The first is to decrease the energy perturbations (motions, cracks, ac losses) as much as possible so that the highest possible operating current can be achieved. This solution can be adopted for small- to medium-scale magnets operating in a *quiet* environment where, for instance, the perturbation energy input can be limited by properly fixing the cable in the winding pack. On the other hand, large size magnets, as typical of SMES systems, thermonuclear fusion experiments or MHD applications, operate in a mechanic and electromagnetic noisy environment (e.g., rapidly changing magnetic fields or large stress cycles) that per force results in a minimum value of the perturbation spectrum. In this case, the designer must increase the stability margin to tolerate the existing perturbation spectrum. This can be achieved by increasing the heat sink associated with the cable.

In the temperature range typical of the operation of a superconducting cable, generally from 2 to 4 K, all solid materials are known to have a very small heat capacity. In the same temperature range, helium uniquely possesses a volumetric heat capacity two to three orders of magnitude larger than solids. Naturally, cable designers tend to take advantage of this feature, trying to make an effective use of the heat sink provided by adding a limited amount of helium to the cable. To achieve this, it is necessary to increase the heat transfer coefficient at the wetted surface of the conductor, at the conductor surface to volume ratio, or both. Forced-flow–cooled conductors are designed along this line to make the most effective use of the helium heat sink.

Stability in forced-flow–cooled conductors is different from classical stability theory in adiabatic and bath-cooled wires, cables, or built-up monoliths mainly for three reasons:

- The largest heat sink providing the energy margin is the helium, and not the enthalpy of the strands themselves or conduction at the end of the heated length.
- This heat sink is limited in amount.
- The helium behaves as a compressible fluid under energy inputs from the strands, implying additional feedback on the heat transfer coefficient through heating induced flow.

The main issue is, therefore, the heat transfer from the strand surface to the helium flow and the thermodynamic process in the limited helium inventory.

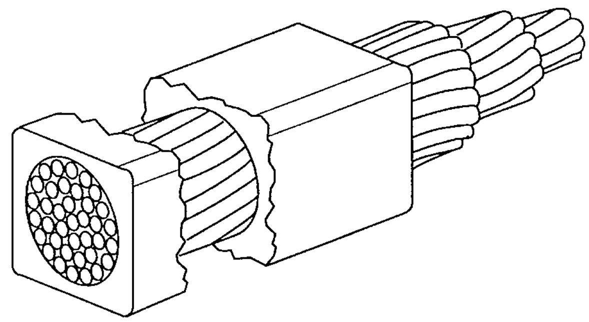

Figure 2. The original concept of CICC, as presented by Hoenig, Iwasa, and Montgomery (7). Reproduced from Ref. 7 by permission of Servizio Documentazione CRE-ENEA Frascati. Copyright 1975 CRE-ENEA Frascati.

FORCED-FLOW–COOLED CONDUCTORS

In a forced-flow conductor, the helium and the superconductor form a single unit, with the coolant flowing inside a pipe also housing the superconductor, or with parallel cooling and electrical paths in close thermal contact. The most common design for this class of conductors is at present the cable-in-conduit conductor (CICC), in which a superconducting cable is placed inside a conduit that also serves as helium containment. We will use this particular type of conductor as a prototype for the general discussion on stability in forced-flow–cooled conductors.

History of Cable-in-Conduit Conductors

The CICC concept evolved from the internally cooled superconductors (ICS), which had found application in magnets of considerable size between the late 60s and early 70s [see in particular the work of Morpurgo (4)]. In ICS, the helium was all contained in the cooling pipe, very much like standard water-cooled copper conductors. The conductor could be wound and insulated using standard technology and the magnet would be stiff both mechanically and electrically, a considerable advantage for medium and large systems requiring, with increasing stored energy, high discharge voltages. Control of the heat transfer and cooling conditions was achieved using supercritical helium, thus avoiding the uncertainties related to a flowing two-phase fluid.

A major drawback of this concept was that according to heat transfer predictions, a large helium massflow would have been required in order to achieve good stability and thus high operating current density. This would require large pumping work and eventually impair the efficiency of the cryogenic system. Chester (5) readily recognized the advantage of the increase in the wetted perimeter obtained by subdivision of the strands. Subdivision dramatically increases the surface-to-volume ratio, thus improving heat transfer for a given cable cross section. Hoenig et al. (6–8) and Dresner (9–11) developed models for the local recovery of ICSs after a sudden perturbation, where they found that for a given stability margin the mass flow required would be proportional to the 1.5th power of the hydraulic diameter as the fixed superconductor inventory is divided in finer and finer strands. This consideration finally brought Hoenig, Iwasa, and Montgomery (6,7) to present the first CICC prototype idea, shown in Fig. 2.

Although many variants have been considered, the basic CICC geometry has changed little since. A bundle conductor is obtained, cabling superconducting strands, with a typical diameter in the millimeter range, in several stages. The bundle is then *jacketed,* that is, inserted into a helium-tight conduit, which provides structural support. Helium occupies the interstitial spaces of the cable. With the cable void fractions of about 30 to 40% commonly achieved, the channels have an effective hydraulic diameter of the order of the strand diameter, while the wetted surface is proportional to the product of the strand diameter and the number of strands. The small hydraulic diameter ensures a high turbulence, while the large wetted surface achieves high heat transfer, so that their combination gives excellent heat transfer properties.

Because of the limited helium inventory, a sufficiently large energy input will always cause a quench in a CICC. This behavior has been defined by Dresner (11,12) as *metastable.* The question is the magnitude of the minimum energy input producing a quench in a particular operating condition. This parameter, the *stability margin* ΔE, was identified by Hoenig (7) as fundamental to the design of a CICC. It is usually measured as an energy per unit strand volume (traditionally expressed in mJ/cm^3). In its original definition, the energy input was thought to happen suddenly, and initial experiments and theory concentrated on this assumption. Throughout this chapter we will use the same definition of the stability margin, extending it to an arbitrary energy deposition time scale.

The heat transfer mechanisms determining stability in supercritical He-I and superfluid He-II are different enough to warrant a separate treatment. The phenomenology of each case and the experimental data supporting the stability calculations are presented in the next sections.

STABILITY MARGIN OF CABLE-IN-CONDUIT CONDUCTORS IN SUPERCRITICAL HELIUM

Dependence on the Mass Flow

Measurements of the stability margin of CICCs in supercritical helium started early in their history (13–19). One of the

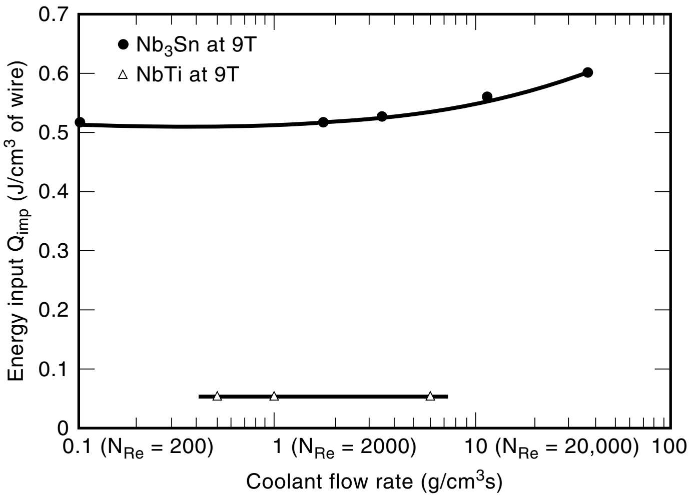

Figure 3. Stability margin of a NbTi and a Nb3Sn CICCs as a function of the steady state helium flow, measured by Hoenig, Montgomery, and Waldman (14). Reproduced from Ref. 14 by permission of IEEE. Copyright 1979 IEEE.

aims was to study the dependence of stability on the coolant flow, to determine the influence of the turbulent heat transfer coefficient and the thermal coupling of strands and helium. The first surprise came with the observation by Hoenig (3) that the stability margin was largely independent of the operating mass flow (see the curves reported in Fig. 3), a result soon duplicated by Lue and Miller (17). These results showed that the heat transfer at the wetted surface of the strands during a temperature excursion was only weakly correlated to the steady state mass flow and the associated boundary layer.

As discussed by Dresner (20) and Hoenig (16), during a strong thermal transient the heat transfer coefficient h at the strand surface changes mainly because of two reasons (see also appendix, Transient Heat Transfer, below):

(a) thermal diffusion in the boundary layer (a new thermal boundary layer is developed and thus h increases compared to the steady state value), and
(b) induced flow (21) in the heated compressible helium (associated with increased turbulence and thus again with an increase in h).

The concurrence of these two effects was advocated to explain the weak dependence of ΔE on the steady mass flow rate.

Dependence on the Operating Current. A second parameter of major interest in the experiments on stability was the operating current of the cable. Several experiments (see the vast amount of data presented in Refs. 22 through 27) have revealed a characteristic behavior of the stability margin as a function of operating current. As we show schematically in Fig. 4, at low operating current a region with high stability margin is observed. We name this region, following Schultz and Minervini (28), the *well-cooled* regime. In this regime, the stability margin is comparable to the total heat capacity available in the cross section of the CICC, including both strands and helium, between operating temperature T_{op} and current-sharing temperature T_{cs}. At increasing current, a fall in the stability margin to low values, the *ill-cooled* regime, is found. In this regime, the stability margin is lower than in the well-cooled regime by typically one to two orders of magnitude, and depends on the type and duration of the energy perturbation.

The transition between the two regimes was identified by Dresner (20) to be at a *limiting* operating current I_{lim}:

$$I_{lim} = \sqrt{\frac{h p_w A_{Cu} (T_c - T_{op})}{\rho_{Cu}}} \quad (2)$$

The above definition of the limiting current I_{lim} is obtained equating the Joule heat generation to the removal at the strand surface, assuming that the helium temperature is constant, and is therefore equivalent to the Stekly criterion of Eq. (1). As discussed later, the heat transfer cofficient h is not constant, but it is a complex function of time and several other parameters such as heating pulse waveform and strength, heating induced flow, and details of the cable design. Let us assume for the moment that the heat transfer coefficient is constant in time and equal to an *effective* value. As shown by Lue (29), it is possible to estimate this effective value of h, deducing it from the location of the limiting current in several experiments. For operating currents below I_{lim} (i.e., in the well-cooled regime), the heat generation is smaller than the heat removal to the helium. A normal zone recovers, provided that the helium is a sufficiently large heat sink capable of absorbing the heat pulse and the subsequent Joule heating. On the other hand, above I_{lim}, in the ill-cooled regime, a normal zone generates more heat than it can exchange to the helium, and therefore recovery is not possible.

This observation indeed explains the behavior of the energy margin below and above I_{lim}. In the well-cooled regime, recovery is unconditional; the cable can transfer a large heat

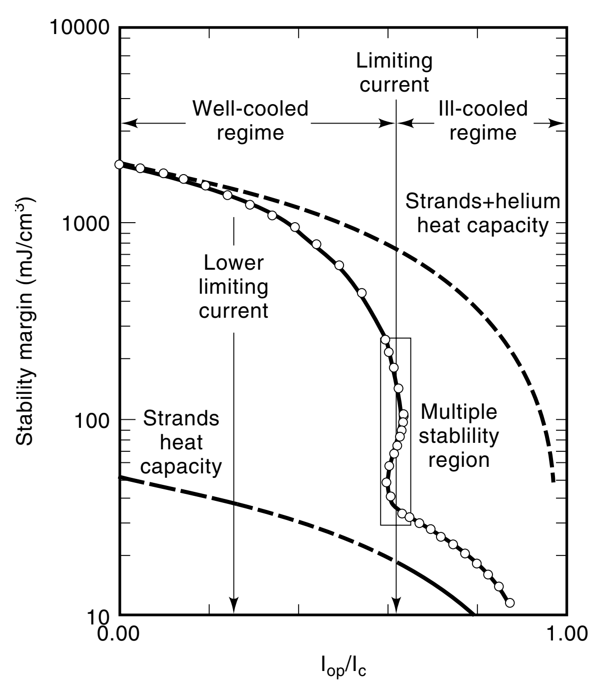

Figure 4. Schematic behavior of the stability margin as a function of the cable operating current.

pulse to the helium and still recover at the end of the pulse, provided that the helium temperature has not increased above T_{cs}. Therefore, the energy margin is of the order of the total heat sink in the cable cross section between the operating temperature T_{op} and T_{cs}, including, obviously, the helium. In the ill-cooled regime, an unstable situation is reached as soon as the strands are current sharing, and therefore the energy margin is of the order of the heat capacity of the strands between T_{op} and T_{cs} plus the energy that can be transferred to the helium during the pulse. As mentioned earlier, in practical cases, the heat capacity of the helium in the cross section of a CICC is the dominant heat sink by two orders of magnitude and more, and this explains the fall in the stability margin above I_{lim}.

The transition between the well-cooled and ill-cooled regimes happens in reality as a gradual fall from the maximum heat sink values to the lower limit [Miller, (25)]. An intuitive explanation of this fall can be given using again the power balance at the strand surface. For the derivation of Eq. (2) it was assumed that the helium has a constant temperature T_{op}. In reality, during the transient, the helium temperature must increase as energy is absorbed and power is transferred under a reduced temperature difference between strand and helium. Two limiting cases can be defined. The first is the ideal condition of helium at constant temperature, giving the limiting current of Eq. (2), for which, however, the energy absorption in the helium is negligible. Operation exactly at I_{lim} results thus in a stability margin at the lower limit—the ill-cooled value. The second limiting case is found when the Joule heat production can be removed even when the helium temperature has increased up to T_{cs}. This second case is obtained for a current of (and below)

$$I_{lim}^{low} = \sqrt{\frac{hp_w A_{Cu}(T_c - T_{cs})}{\rho_{Cu}}} \tag{3}$$

that we call *lower limiting current* for analogy to Eq. (2) and because I_{lim}^{low} is always smaller than I_{lim}. For operation at (and below) I_{lim}^{low}, the full heat sink can be used for stabilization and the stability margin is at the upper limit—the well-cooled value. Between the two values I_{lim} and I_{lim}^{low}, the stability margin falls gradually.

Multiple Stability

Near the limiting current the balance between heat production and removal becomes critical. Indeed, in some cases, a multivalued region can be found in the vicinity of I_{lim}, as schematically shown in Fig. 4. As mentioned earlier, supercritical helium behaves as a compressible fluid in the typical range of operation of a magnet. Therefore, any heat pulse causes a heating-induced flow driven by the fluid expansion and proportional to the pulse power. The flow in turn modifies the heat transfer at the wetted surface of the conductor, enhancing the heat transfer coefficient. Let us concentrate on the close vicinity of the limiting current, just above I_{lim} on the ill-cooled side. A large heating power, above the ill-cooled stability margin, can result in a significant heating-induced flow and thus a large enhancement of the heat transfer coefficient. Hence the power balance can be tipped in the direction favorable to recovery, and a second stable region appears. This is what has been observed by Lue, Miller and Dresner (18,19)

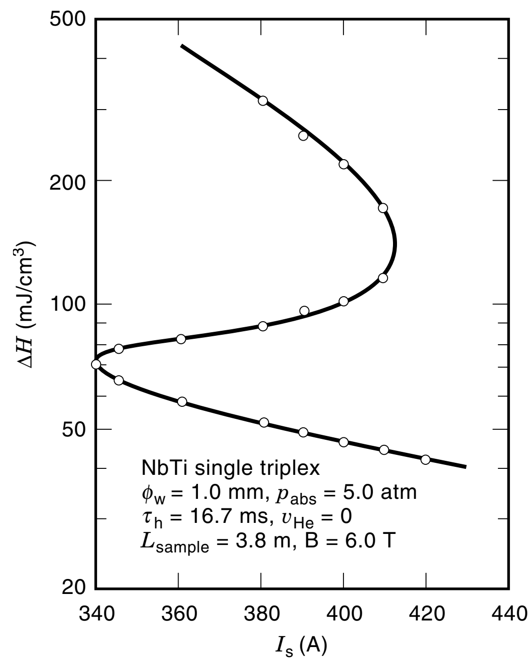

Figure 5. Stability margin of a NbTi CICC as a function of the operating current, measured by Lue and Miller (19). The experiment was performed on a single triplex CICC of 3.8 m length (L_{sample}), with strand diameter of 1 mm (ϕ_w), under zero imposed flow (v_{He}) at a helium pressure of 5 bar (p_{abs}). The background field was 6 T (B), and resistive heating took place in 16.7 ms (τ_h). Reproduced from Ref. 19 by permission of IEEE. Copyright 1981 IEEE.

in experiments on single triplex NbTi cables. Figure 5 reports one such multiple stability curve, as measured as a function of the operating current. This situation is evidently not agreeable for reliable operation and should be avoided in a sound design by remaining safely below the limiting current.

Dependence on the Operating Field

The stability margin is a function of the background field B mainly through the dependence on critical and current-sharing temperatures. A higher B causes a drop both in the limiting current (through a decrease of T_c and increase of ρ_{Cu}) and in the energy margin (through a decrease in T_{cs}). Therefore, ΔE drops as the field increases. An interesting feature is that the limiting current only decreases with $(T_c - T_{op})^{1/2}$, that is, with a dependence on B weaker than that of the critical current. At large enough B we will always have that I_{lim} is larger than I_c and the cable will reach the critical current while still under well-cooled conditions.

Dependence on the Heating Time Scale. The stability margin depends on the duration of the heating pulse, as shown experimentally by Miller et al. (17), and reported here in Fig. 6. A change in the heating duration for a given energy input corresponds to a change in the pulse power. In the well-cooled regime, that is, for low operating currents in Fig. 6, the heat balance at the end of the pulse is in any case favorable to recovery, and therefore the energy margin does not show any significant dependence on the pulse duration. On the other hand, when the conductor is in the ill-cooled regime, its temperature can increase to or slightly beyond T_{cs} without caus-

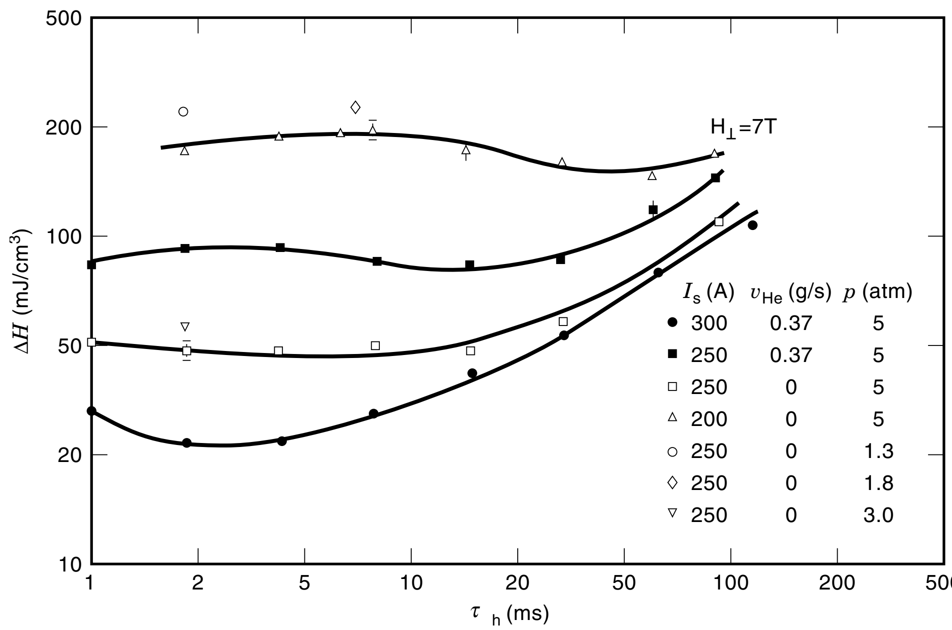

Figure 6. Dependence of the stability margin for a CICC (indicated on this plot as ΔH) on the heating time scale (τ_h), as measured by Miller et al. (17). The parameters varied in the experiment, indicated in the inset, are the transport current in the sample I_s, the helium flow velocity v_{He}, and the pressure p. Reproduced from Ref. 17 by permission of IEEE. Copyright 1979 IEEE.

ing a quench. This limits the heat flux per unit length at the wetted surface to roughly $hp_w(T_{cs} - T_{op})$. The consequence is that energy transferred to the helium, and thus the energy margin, will grow at increasing pulse duration, until it becomes comparable to the total heat capacity available (as in the well-cooled regime). This effect is partially balanced for very fast pulses, because the heat transfer coefficient can exhibit very high values at early times (see the appendix, Transient Heat Transfer, below), which could shift the well-cooled/ill-cooled transition at higher transport currents. In principle, higher energy margins should be expected in this range. However, the high input powers in this duration range tend to heat the conductor above 20 K, in a temperature range where the stabilizer resistivity grows quickly, and the power balance is thus strongly influenced. This effect causes the saturation of the energy margin for extremely fast pulses (well below 1 ms duration).

Dependence on Operating Temperature and Pressure

The dependence on the operating temperature and pressure in supercritical conditions is not easily quantified. The reason is that the helium heat capacity in the vicinity of the usual regimes of operation (operating pressure p_{op} of the order of 3 to 10 bar and operating temperature T_{op} around 4 to 6 K) varies strongly with both p_{op} and T_{op}. This affects both the heat sink and the heat transfer coefficient (through its transient components). An increasing temperature margin under constant operating pressure gives a higher ΔE. But a simultaneous variation of p_{op} and T_{op}, under a constant temperature margin, can produce variations of ΔE as large as a factor two in the range given above [see Miller (25) and Chaniotakis, (30)].

STABILITY MARGIN OF CABLE-IN-CONDUIT CONDUCTORS IN SUPERFLUID HELIUM

If the operating temperature is lowered below the so-called *lambda* value T_λ (e.g., 2.17 K at 1 atm), helium undergoes a state change and becomes a quantum fluid: *superfluid* helium, or He-II. He-II has unique properties and its physical behavior is very different from that of *normal* helium (or He-I). For our purposes, the most remarkable fact is that He-II does not obey the traditional Fourier law of conduction (proportionality between heat flux and temperature gradient), but rather follows a nonlinear law of the form

$$q = -K(\nabla T)^{1/3} \tag{4}$$

where q is the heat flux, K is a parameter that depends on the thermodynamic state of the He-II, and ∇T is the temperature gradient. For heat fluxes of practical interest, the He-II properties are such that the “equivalent thermal conductivity” is extremely high, orders of magnitude higher than in He-I. “Superfluid heat conduction” refers to the ability of stagnant He-II to provide significant heat removal over long lengths of narrow channels without an appreciable temperature gradient, making it an attractive alternative for superconducting magnet cooling (31,32).

Similarly to the behavior in He-I, the stability margin of a CICC operating in He-II is determined by the balance between Joule heating and the ability of the helium to provide enough enthalpy margin, given that metal-to-helium heat transfer is sufficient. Lottin and Miller (27) have measured stability margin of a CICC at different operating temperatures, both in supercritical and superfluid helium. We show typical results of this experiment in Fig. 7. The stability margin behaves at low current in a way similar to what would be expected in the case of He-I operation. However, at the ill-cooled transition—the first drop in the stability curve taking place at similar currents both in He-I and He-II—the stability margin shows a peculiar behavior. Owing to the large heat transfer capability in He-II, the power balance at the strand surface remains favorable for recovery as long as the bulk helium is in the He-II phase. Therefore, in a first approximation, the full heat sink between the initial operating point and the transition temperature T_λ is still available at levels of the

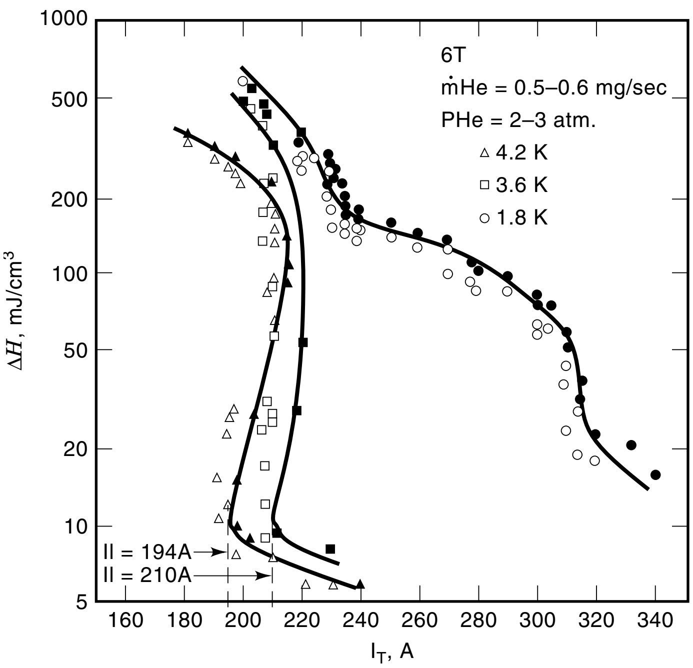

Figure 7. Stability margin of a NbTi CICC as a function of the operating current, measured by Lottin and Miller (27), at different temperatures in supercritical and superfluid helium (filled-in symbols are quenches, open symbols are recoveries). Reproduced from Ref. 27 by permission of IEEE. Copyright 1983 IEEE.

operating current at which the conductor would have turned to be ill-cooled for operation in He-I. In other words, the conductor can still be considered as *well-cooled* for temperature excursions up to T_λ. We can call this region of operation the *superfluid* stability regime. As the helium undergoes a phase transition at the temperature T_λ, the available heat sink is significant, of the order of 200 mJ/cm^3 of helium volume. At increasing current, finally, the power balance can eventually become unfavorable, as soon as the heat removal capability of He-II reaches its upper limit. There the final transition to the ill-cooled regime of operation takes place. Unlike the He-I case, the transition from high to low stability-margin regimes occurs gradually without a region of multivalued stability owing, on the one hand, to a small coefficient of thermal contraction (compared to the large thermal expansion in He-I), and, on the other hand, to a very high effective thermal conductivity of He-II, both preventing the onset of large heating induced flows.

In the *superfluid* well-cooled stability regime, where the conductor takes advantage of the superfluid helium properties only, the stability margin has a distinct behavior (33–37) that, as indicated by Seyfert, Laffarranderie, and Claudet (33), is mainly determined by the near-field effects of surface heat transfer to He-II. Following a disturbance, the metal temperature exceeds T_λ almost immediately, and the helium in contact with the strand undergoes the transition to He-I. However, at some distance from the strand surface, there is an He-I/He-II transition where the temperature is T_λ. It can be shown that, given the heat transfer properties of He-II, the layer of He-I adjacent to the strand is negligibly thin (33). The consequence is that, for all practical purposes, heat transfer in the superfluid bath takes place "as if" the strand surface had its temperature clamped at T_λ. This is indeed the basis for the simplified model used to calculate the heat flux limits in He-II and the behavior of the stability margin in the superfluid region.

CALCULATION OF THE STABILITY MARGIN IN HE-I

The calculation of the stability margin in a CICC is a difficult task, involving accurate computation of compressible helium flow and heat diffusion in a complex geometry. For practical purposes, several simplified models have been developed. These models make extensive use of the experimental evidence discussed in the previous sections as a basis for introducing and justifying several simplifications. For the purpose of introducing the reader to the concepts involved in the calculation of the energy margin, this presentation will start with a very simplified model (an integrated energy balance), and then proceed to introduce refinements to the model [a zero-dimensional (0-D) energy balance model, and a one-dimensional (1-D) flow model].

Energy Balance

The simplest stability model is that considering the energy balance for the combined helium/strand system integrated over the duration of the disturbance. This method gives a rough estimate of the stability margin in the well- and ill-cooled regimes (called here ΔE_{wc} and ΔE_{ic}) based on the available heat capacities and the location of the well-cooled/ill-cooled boundary (neglecting the dual-stability region), and has the advantage of producing easily applicable design criteria for the selection of the cable layout. We introduce the maximum heat sink in the cable cross section (referred to the unit strand volume) ΔE_{max}:

$$\Delta E_{\max} = \int_{T_{op}}^{T_{cs}} \frac{A_{He}}{A_{St}} C_{He}\, dT + \int_{T_{op}}^{T_{cs}} C_{St}\, dT \qquad (5)$$

where C_{He} and C_{St} are respectively the volumetric heat capacity of helium and of the strands, while A_{He} and A_{St} are their cross sections. The estimate of C_{He} can pose some questions. As known from thermodynamics, the volumetric heat capacity in a compressible fluid depends on the process assumed. Two limiting cases can be identified: a process at constant volume, where we have that $C_{He} = \rho c_v$; or the case of constant pressure, where we have that $C_{He} = \rho c_p$ (c_v and c_p represent the helium constant-volume and constant-pressure–specific heat). The proper selection depends on the comparison of the characteristic times involved. In a transient where the flow characteristic times are much longer than the heating and recovery time (i.e., for long-heated zone or fast-heating pulse), the process will be at constant volume. Approximate constant pressure conditions will be found when the flow characteristic times are much shorter than the heating time (short heated zone or long pulse). The real process will be between these two extremes, but generally a conservative estimate is obtained choosing the constant volume process.

In the well-cooled regime we will have

$$\Delta E_{wc} \le \Delta E_{\max}$$

that is, the energy margin is at most equal to the available heat sink up to T_{cs}, and in general smaller than ΔE_{max}. A first reason is that during the heat pulse τ_e and the recovery time τ_r, the Joule heat generated by the current sharing strand consumes the available heat capacity. An approximation of the Joule heat contribution normalized to the strand volume is given by

$$Q_{\mathrm{Joule}} = \int_0^{\tau_e+\tau_r} \frac{\rho_{\mathrm{Cu}} I^2}{A_{\mathrm{Cu}} A_{\mathrm{St}}}\, dt \tag{6}$$

This contribution increases at increasing operating current and increasing energy deposition time, although the above approximation tends to give only an upper limit and overestimates the real contribution (the strands are assumed fully normal for the whole transient). Still, for fast and for most common heating pulses (typically in the 1 to 10 ms range) the term above is small. It is then justifiable to neglect the gradual fall of ΔE, and to take

$$\Delta E_{\mathrm{wc}} \approx \Delta E_{\mathrm{max}} \tag{7}$$

For operation in the ill-cooled regime at and above I_{lim}, the energy margin can be approximated as the sum of the strand heat capacity up to T_{cs} and the energy transferred from the strand to the helium during the heat pulse (38), again expressed per unit of strand volume:

$$\Delta E_{\mathrm{ic}} \approx \int_{T_{\mathrm{op}}}^{T_{\mathrm{cs}}} C_{\mathrm{St}}\, dT + \frac{p_{\mathrm{w}}}{A_{\mathrm{St}}}(T_{\mathrm{cs}} - T_{\mathrm{op}}) \int_0^{\tau_e+\tau_r} h dt \tag{8}$$

where the second term on the right-hand side is an approximation of the energy transferred to the helium under the assumption that the strands rise instantaneously to T_{cs} and the helium temperature T_{op} does not change significantly. For short energy pulses, the use of Eq. (8) shows that generally $\Delta E_{ic} \ll \Delta E_{max}$. The energy margin given by Eq. (8) tends to increase when the energy deposition time τ_e increases, which is consistent with the experimental results quoted earlier. For very long pulses, the power input in the strand can be transferred to the helium without a significant temperature difference. At the limit of long pulse times, the whole heat capacity is used again and we have that $\Delta E_{ic} \approx \Delta E_{max}$. In any case, the value of the maximum heat sink ΔE_{max} of Eq. (5) remains the absolute upper limit of the stability margin. In summary, Eqs. (7) and (8) give the estimated energy margin respectively below and above the limiting current of Eq. (2).

Zero-Dimensional Model

The next level of complexity and accuracy in the calculation of the stability margin consists of introducing time as a variable to capture the distinction between short and long duration pulses while neglecting heated-zone length effects. Maintaining the fundamental distinction between strand and helium temperature, it is possible to write this 0-D balance as follows:

$$A_{\mathrm{St}} C_{\mathrm{St}} \frac{\partial T_{\mathrm{St}}}{\partial t} = \dot{q}'_{\mathrm{Ext}} + \dot{q}'_{\mathrm{Joule}} - p_{\mathrm{w}} h (T_{\mathrm{St}} - T_{\mathrm{He}}) \tag{9a}$$

$$A_{\mathrm{He}} C_{\mathrm{He}} \frac{\partial T_{\mathrm{He}}}{\partial t} = p_{\mathrm{w}} h (T_{\mathrm{St}} - T_{\mathrm{He}}) \tag{9b}$$

The rightmost terms in Eqs. (9a) and (9b) represent the thermal coupling of strands (at temperature T_{St}) and helium (at temperature T_{He}) at the wetted perimeter p_w with a heat transfer h. In Eq. (9a) we have in addition the external and Joule heat sources (per unit conductor length) $\dot{q}'_{Ext}$ and $\dot{q}'_{Joule}$, respectively. The Joule heating can be computed once the critical current dependence on the temperature $I_c(T)$ is known. Note that an accurate calculation of $\dot{q}'_{Joule}$ is necessary to describe the recovery phase properly. This model is attractive because of its simplicity; it can be solved efficiently and used routinely. It is accurate in describing the local energy balance on the time scale of recovery, but some care must be taken in the selection of the parameters in order to capture flow-related physical features that only a 1-D model can include.

The first parameter to be chosen properly is the volumetric helium heat capacity, as we discussed earlier. The second parameter that requires care is the heat transfer coefficient, changing in time during the transient. While the boundary layer formation and the associated diffusive component of the heat transfer coefficient can be approximated in a local treatment as a variable thermal resistance between strands and helium, the heating-induced flow and its effect on stability are not amenable to local treatment. An average value for this component is a reasonable choice, but the actual modeling is to a large extent left to empiricism [see Lue (29)]. This is, in fact, one of the research areas on stability margin in CICCs.

The search of the stability margin with the 0-D model is the *virtual* analogue of the experimental technique. A trial-and-error search is done on the energy input, increasing or decreasing it as a function of the quench or recovery result at the end of the transient.

One-Dimensional Model

With a typical hydraulic diameter in the millimeter range, the overall helium flow in a CICC can be expected to be one-dimensional, with a good approximation already over flow lengths of the order of 1 m. As the helium flows generally in turbulent regime, the helium temperature is nearly uniform in the cross section of the CICC. Therefore, the temperature gradients in the cable cross section reduce to those across the strand, and are negligibly small. We assume that the current distribution is uniform in the strands. In well-designed CICCs, the current can redistribute over typical lengths of the order of some centimeters in times of the order and below 1 ms. In this case, the heat generation in the CICC cross section during current sharing is also uniform. This is not the case for CICCs with insulated strands or high transverse resistance, where the current redistribution can take several seconds over lengths of several meters. In this case, an homogenized treatment is not appropriate and the stability margin is actually strongly degraded. We will therefore drop this case in the following treatment. As the stability transients are fast compared to the thermal diffusivity of the conduit materials (e.g., steel), the conduit contribution to the energy balance is neglected also.

These assumptions lead to a much simplified 1-D model of the CICC, where two constituents are identified: the helium and the strands. Both are at uniform, but distinct, temperature. The compressible flow equations in the helium (mass, momentum, and energy balances) are written to include wall friction, modeled using a turbulent friction factor. Strand and helium exchange heat at the wetted surface, and the thermal coupling is usually modeled using the correlation for the heat transfer coefficient h discussed in Appendix. The system is then described by the equations:

$$\frac{\partial \rho}{\partial t} + \frac{\partial \rho v}{\partial x} = 0 \tag{10a}$$

$$\frac{\partial \rho v}{\partial t} + \frac{\partial \rho v^2}{\partial x} + \frac{\partial p}{\partial x} = -2\rho f \frac{v|v|}{D_\mathrm{h}} \tag{10b}$$

$$\frac{\partial \rho e}{\partial t} + \frac{\partial \rho v e}{\partial x} + \frac{\partial p v}{\partial x} = \frac{p_w h}{A_\mathrm{He}}(T_\mathrm{St} - T_\mathrm{He}) \tag{10c}$$

$$A_\mathrm{St} C_\mathrm{St} \frac{\partial T_\mathrm{St}}{\partial t} - A_\mathrm{St} \frac{\partial}{\partial x}\left(K_\mathrm{St} \frac{\partial T_\mathrm{st}}{\partial x}\right) = \dot{q}'_\mathrm{Ext} + \dot{q}'_\mathrm{Joule} - p_w h (T_\mathrm{St} - T_\mathrm{He}) \tag{10d}$$

where ρ is the helium density, p its pressure and v is the flow velocity, f the friction factor and D_h is the hydraulic diameter of the conductor. The total specific energy e is defined as the sum of the internal specific energy i and the kinetic specific energy, that is,

$$e = i + \frac{v^2}{2}$$

Finally, the strand heat balance of Eq. (10d) takes into proper account the contribution of the heat conductivity K_St along the cable length.

The 1-D model introduced above is widely used for detailed calculations of stability margin. When the numerical solution technique to account for the different time scales involved is properly selected, the model can predict the heating-induced flows responsible for multivalued stability, and can be adapted directly to follow the evolution of the normal zone when the energy input is large enough and the coil quenches. The only significant modification in this case is the need to take into account the additional heat capacity of the conduit material. This modification is straightforward and consists of adding a temperature diffusion equation to the system. Because of the level of fine details, even within the simplification of the 1-D assumption, this model gives the possibility of wide parametric analysis. Its main drawback is that, dealing with largely different time scales, it is slow and not easy to handle.

CALCULATION OF STABILITY MARGIN IN HE-II

A CICC operating in superfluid helium is most efficient if it is designed to take advantage of the large heat removal capability at the strand wetted surface. As we discussed in the description of the general features of the stability margin in He-II, it is possible to operate the cable at a current density significantly higher than in the case of supercritical helium. However, we recall that in the *superfluid* well-cooled regime, the upper stability margin is determined by the helium enthalpy available between operating temperature and the lambda point, of the order of 200 mJ/cm^3 of helium volume. Therefore, in the design for operation in He-II, we assume implicitly that if the Joule heating is enough to drive the bulk temperature above T_λ, cooling in He-I is so reduced in relation to superfluid cooling that the conductor will not recover.

As for operation in supercritical He-I, the stability margin of a CICC in He-II can be computed at different levels of approximation and complexity. We need in this case to modify the heat transfer coefficient (see the Appendix) and the helium energy balance to take into account the equivalent thermal conductivity given by Eq. (4). However, the model used in practice to design CICCs for stable operation in He-II is different from that discussed in the previous section. In this case, we concentrate on the heat removal capability, with the aim of maintaining it sufficiently high so that the full helium heat sink up to the lambda point is available for stabilization.

The essence of the simplified model, due to Dresner (36,37), consists in solving the 1-D heat transport equation in stagnant He-II in a channel in order to obtain the effective cooling capacity. The model implies that even if the helium goes through the lambda transition at the conductor surface, the bulk of the coolant remains in the superfluid state and cooling is determined by "conduction" along the channel (in the case of a CICC, the "channel" is the imaginary annulus of helium surrounding each strand). This is consistent with Seyfert's observation that the layer of He-I around each strand is negligibly thin (33). Dresner's model is based on the analytical solution of the nonlinear heat "conduction" in the annulus of He-II around the strands, and the ability of the helium to absorb the heat flux stemming from the Joule heating (for details of the derivation see Refs. 36 and 37). In that context, it is useful to define the following two quantities:

$$E = \frac{A_{Cu}}{p_\mathrm{w}} \Delta E \tag{11a}$$

$$E_\mathrm{o} = \left[h_\mathrm{He}(T_\lambda) - h_\mathrm{He}(T_\mathrm{op})\right] L \tag{11b}$$

where the quantity E is just a different scaling of the stability margin (the quantity of interest in this calculation), h_He is the helium enthalpy per unit volume, and L is the effective "channel" length, so that E_o represents the maximum enthalpy available between the operating temperature and the lambda temperature in the annulus of helium around each strand (the total heat sink). The equivalent channel length L depends on the helium cross section as follows:

$$p_\mathrm{w} L = A_\mathrm{He} = \frac{f_\mathrm{He}}{1 - f_\mathrm{He}} A_\mathrm{St} \tag{11c}$$

where f_He is the CICC void fraction. The analytical solution of the Dresner model leads to a relationship between the stability margin and the design current density that can be expressed using the nondimensional groups E/E_o and q_j/q^*, with the latter terms defined as follows:

$$q_j = \frac{\rho_\mathrm{Cu} I^2}{p_\mathrm{w} A_\mathrm{Cu}} \tag{11d}$$

$$q^* = \frac{K C_\mathrm{He}^{1/3} (T_\lambda - T_\mathrm{op})^{2/3}}{(4E_\mathrm{o})^{1/3}} \tag{11e}$$

in which q_j represents the Joule heating in the cable per unit of cooling surface. The quantity q^* is a fiducial heat flux that depends on the effective thermal conductivity of superfluid helium (K), the volumetric specific heat of the helium (C_He), the temperature difference between the operating point and the lambda transition, and E_o (defined above). This quantity

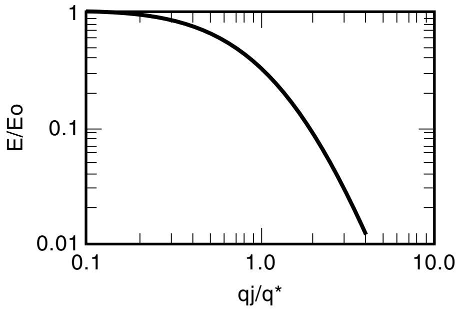

Figure 8. Semiempirical representation of the stability margin for a CICC operating in He-II.

stems from the solution of the nonlinear heat conduction equation for He-II. The ratio q_j/q^* determines the severity of the Joule heating pulse that needs to be transported and absorbed by the superfluid helium.

The model predicts an expression relating E/E_o as a function of q_j/q^*, which is shown in Fig. 8. The results of this stability model indicate that, as in He-I operation, there are two distinct regimes: at low currents the conductor is *well-cooled* and essentially the entire helium enthalpy margin (up to the transition to He-I) is available to stabilize the cable; at higher currents the cable becomes *ill-cooled* and the stability margin is significantly lower because of the inability of the He-II to conduct the Joule heat flux over the length of the equivalent "channel."

The criterion used in practice then stems directly from the results of this model. To ensure the highest possible stability margin (the entire helium enthalpy from the operating point to the lambda point), the conductor needs to be designed so that $q_j = 0.2q^*$, for at higher fractions of q^* the margin decreases rapidly. Note that as a result, the conductor design (and the stability margin) depends only on the physical properties of the He-II and on the current density in the stabilizer. The current sharing temperature does not enter into the determination of stability as a result of assuming that the conductor cannot recover once the lambda transition is crossed during a disturbance. The present model has been successfully used in the design of a large (200 kA) CICC for application in SMES (39,40).

CONCLUSIONS AND RESEARCH DIRECTIONS

This article has presented the basic considerations and models that go into the design of CICCs for stable operation. Enough is known of the mechanisms determining stability so that, in conjunction with other constraints, CICCs can be designed successfully and even optimized (41). However, this does not mean the field is not open to new areas of research. As new magnet designs are proposed, and as more stringent requirements are imposed on the designer, areas of further study continue to open—in particular, work toward improving our understanding of stability under transient operating conditions (e.g., ac losses and stability) or for more complex cable geometries (e.g., CICC with central channels).

As may be clear after review of the literature, stability depends in a synergistic manner on the dc and ac operating conditions of the cable in the coil (42–44). This is the main direction of the actual research in the field of CICC stability. In particular, in view of the applications to pulsed magnets, the interaction of stability, current distribution, and ac losses in the cable is one of the main topics. The so-called *ramp-rate* limit of operation for pulsed magnets (43–45) (a decrease in the maximum achievable current at increasing field change rate) is an outstanding example of this synergistic interaction. The appearance of such a phenomenon, explained so far in terms of nonuniform current distribution and a degradation of the stability margin of the cable, has alerted us to the difference between dc stability, with constant operating current and background field, and ac stability of the cable.

However, while dc operating conditions are easier to produce and simulate, ac stability is difficult to measure and poses some basic problems in the interpretation of the data. The simulation and prediction of ac stability are therefore object of an intense activity in the field of transient electromagnetics in superconductors and thermohydraulics.

APPENDIX: TRANSIENT HEAT TRANSFER

The main issue in heat transfer is fast transients, for their relevance to stability. A strong variation of the transient heat transfer to a flow of supercritical helium was demonstrated by Giarratano (46) and Bloem (47) in dedicated measurements on short test sections. The experiments showed an initial peak in the heat transfer coefficient at early times, below 1 ms. At later times, in the range of some ms to about 100 ms, the initial peak decreased approximately with the inverse of the square root of time. This behavior could be explained in terms of the diffusion of heat in the thermal boundary layer. Using the analytical solution of diffusion in a semi-infinite body (the helium) due to a heat flux step at the surface, the effective heat transfer coefficient can be computed as [Bloem (47)]:

$$h_t = \frac{1}{2}\sqrt{\frac{K_{\mathrm{He}}\rho c_{\mathrm{p}}}{\pi t}} \tag{12}$$

where K_{He} is the heat conductivity of helium. The expression above is shown to fit properly the experimental data for times longer than 1 ms and until the thermal boundary layer is fully developed. At earlier times, Eq. (12) would tend to predict an exceedingly high heat transfer coefficient, consistent with the assumptions of the analytical calculation. In reality, the early values of h are found to be limited by the Kapitza resistance (48) at the contact surface of strand and helium, which gives a significant contribution only when the transient heat transfer coefficient is in the order of or larger than 10^4 W m^{-2} K (or in the case that the wetting helium is in the superfluid state). A suitable expression for the heat transfer coefficient in the Kapitza resistance can be obtained using

$$h_{\mathrm{K}} = 200(T_{\mathrm{St}}^2 + T_{\mathrm{He}}^2)(T_{\mathrm{St}} + T_{\mathrm{He}}) \tag{13}$$

which, in fact, approximates a radiation-like phenomenon at the conductor surface with an equivalent heat transfer coefficient (T_{St} and T_{He} are the strand and the helium temperature, respectively).

At later times, usually around 10 to 100 ms, the thermal boundary layer is fully developed and the steady state value of h is approached. Its value appears to be well approximated by a correlation of the Dittus-Boelter form, as shown by Yaskin (49) and Giarratano (50). A best fit of the available data is obtained with the following expression (neglecting corrections due to large temperature gradients at the wetted surface):

$$h_\mathrm{s} = 0.0259\frac{K_\mathrm{He}}{D_\mathrm{h}}\mathrm{Re}^{0.8}\mathrm{Pr}^{0.4} \tag{14}$$

An empirical expression for the heat transfer to supercritical helium during a transient finally can be obtained modeling the Kapitza resistance and the helium boundary layer as series thermal resistances, and taking

$$h = \max\left\{\frac{h_t h_K}{h_t + h_K}, \frac{h_s h_K}{h_s + h_K}\right\} \tag{15a}$$

This expression is in good agreement with the experimental results quoted above, and shows that, for short pulses, the heat transfer coefficient only depends on the helium state and not on the flow conditions. At temperatures below the lambda point (superfluid helium), the Kapitza resistance is the only limit to the heat transfer at the strand wetted surface. In this case, we approximate the heat transfer coefficient simply as

$$h = h_K \tag{15b}$$

Equations (15a) and (15b) can then be used to approximate the heat transfer coefficient at the strand-helium interface for the entire transient in the supercritical regime, or to cover the entire operating temperature range, from below the lambda point to 4.2 K and above. It should be noted, however, that the expressions above are only a convenient tool to implement in stability models covering most regimes of interest, and do not capture all the complexities encountered, for instance, when operating in atmospheric superfluid, when phase changes may be taking place at the interface during a transient.

BIBLIOGRAPHY

1. Z. J. J. Stekly and J. L. Zar, Stable superconducting coils, *IEEE Trans. Nuc. Sci.,* **12**: 367, 1965.
2. V. E. Keilin, Explanation of main features of superconducting windings training by balance of acting and permissible disturbances, *IEEE Trans. Appl. Supercond.,* **3**: 297–300, 1993.
3. V. E. Keilin, An approach to deduce quench fields of superconducting magnets from model coils testings, *IEEE Trans. Magn.,* **30**: 1962–1965, 1994.
4. M. Morpurgo, The design of the superconducting magnet for the "Omega" project, particle accelerators, vol. I, Glasgow, UK: Gordon and Breach Publishers (printed by Bell and Bain Ltd.), 1970.
5. P. F. Chester, Superconducting magnets, *Reports on Progress in Physics,* **XXXII**: 561–614, 1967.
6. M. O. Hoenig and D. B. Montgomery, Dense supercritical helium cooled superconductors for large high field stabilized magnets, *IEEE Trans. Magn.,* **11**: 569, 1975.
7. M. O. Hoenig, Y. Iwasa, and D. B. Montgomery, Supercritical-helium cooled "bundle conductors" and their application to large superconducting magnets, *Proc. 5th Int. Conf. Magn. Tech.,* Rome, Italy, 21–25 Apr. 1975, in N. Sacchetti, M. Spadoni, and S. Stipcich (eds.), Frascati Lab. Naz. del CNEN, 519, 1975.
8. M. O. Hoenig et al., Supercritical helium cooled cabled, superconducting hollow conductors for large high field magnets, *Proc. 6th Int. Cryo. Eng. Conf.,* Grenoble, France, 11–14 May 1976, in K. Mendelssohn (ed.), Guilford, Surrey 1PC Science and Technology Press, 310, 1976.
9. L. Dresner, Stability-optimized, force-cooled, multifilamentary superconductors, *IEEE Trans. Magn.,* **13**: 670, 1977.
10. L. Dresner and J. W. Lue, Design of forced-cooled conductors for large fusion magnets, *Proc. 7th Symp. on Eng. Probs. of Fus. Res.,* **I**: 703, 1977.
11. L. Dresner, Stability of internally cooled superconductors: A review, *Cryogenics,* **20**: 558, 1980.
12. L. Dresner, Superconductor stability 1983: A review, *Cryogenics,* **24**: 283, 1984.
13. M. O. Hoenig and D. B. Montgomery, Cryostability experiments of force cooled superconductors, *Proc. 7th Symp. on Eng. Probs. of Fus. Res.,* **I**: 780, 1977.
14. M. O. Hoenig, D. B. Montgomery, and S. J. Waldman, Cryostability in force cooled superconducting cables, *IEEE Trans. Magn.,* **15**: 792, 1979.
15. M. O. Hoenig, Internally cooled cabled superconductors—Part I, *Cryogenics,* **20**: 373–389, 1980.
16. M. O. Hoenig, Internally cooled cabled superconductors—Part II, *Cryogenics,* **20**: 427–434, 1980.
17. J. R. Miller et al., Measurements of stability of cabled superconductors cooled by flowing supercritical helium, *IEEE Trans. Magn.,* **15**: 351, 1979.
18. J. W. Lue, J. R. Miller, and L. Dresner, Stability of cable-in-conduit superconductors, *J. Appl. Phys.,* **51**: 772, 1980.
19. J. W. Lue and J. R. Miller, Parametric study of the stability margin of cable-in-conduit superconductors: Experiment, *IEEE Trans. Magn.,* **17**: 1981.
20. L. Dresner, Parametric study of the stability margin of cable-in-conduit superconductors: Theory, *IEEE Trans. Magn.,* **17**: 753, 1981.
21. L. Dresner, Heating induced flows in cable-in-conduit conductors, *Cryogenics,* **19**: 653, 1979.
22. J. R. Miller et al., Stability measurements of a large Nb_3Sn force-cooled conductor, *Adv. Cryo. Eng.,* **26**: 654, 1980.
23. J. W. Lue and J. R. Miller, Performance of an internally cooled superconducting solenoid, *Adv. Cryo. Eng.,* **27**: 227, 1982.
24. J. V. Minervini, M. M. Steeves, and M. O. Hoenig, Experimental determination of stability margin in a 27 strand bronze matrix, Nb_3Sn cable-in-conduit conductor, *IEEE Trans. Magn.,* **21**: 339, 1985.
25. J. R. Miller, Empirical investigation of factors affecting the stability of cable-in-conduit superconductors, *Cryogenics,* **25**: 552, 1985.
26. T. Ando et al., Investigation of stability in cable-in-conduit conductors with heat pulse duration of 0.1 to 1 ms, *Proc. 11th Int. Cryo. Eng. Conf.,* 756, 1986.
27. J. C. Lottin and J. R. Miller, Stability of internally cooled superconductors in the temperature range 1.8 to 4.2 K, *IEEE Trans. Magn.,* **19**: 439, 1983.
28. J. H. Schultz and J. V. Minervini, Sensitivity of energy margin and cost figures of internally cooled cabled superconductors (ICCS) to parametric variation in conductor design, *Proc. 9th Magn. Tech. Conf.,* 643–646, 1985.
29. J. W. Lue, Review of stability experiments on cable-in-conduit conductors, *Cryogenics,* **34**: 779–786, 1994.
30. E. A. Chaniotakis, Energy margin of cable-in-conduit conductor as a function of operating pressure and initial heated zone, *IEEE Trans. Magn.,* **32** (4): 2966–2969, 1996; also E. A. Chanionakis,

Effect of operating pressure and heated length on the stability of CICCs, *J. Fusion Energy,* **14** (1): 69–73, 1995.

31. G. Claudet et al., Superfluid helium for stabilizing superconductors against local disturbances, *IEEE Trans. Magn.,* **15**: 340, 1979.
32. S. W. Van Sciver, Stability of superconductors cooled internally by He II heat transfer, *Cryogenics,* **31**: 516, 1991.
33. P. Seyfert, J. Laffarranderie, and G. Claudet, Time-dependent heat transport in subcooled superfluid helium, *Cryogenics,* **22**: 401, 1982.
34. C. Meuris et al., Transient stability of superconductors cooled by superfluid helium at atmospheric pressure, *Proc. Int. Inst. Refrigeration,* 215–223, 1981.
35. C. Meuris, Experimental study of the stability of a superconductor cooled by a limited volume of superfluid helium, *IEEE Trans. Magn.,* **19**: 272, 1983.
36. L. Dresner, A rapid, semiempirical method of calculating the stability margins of superconductors cooled with subcooled He-II, *IEEE Trans. Magn.,* **23**: 918–921, 1987.
37. L. Dresner, *Stability of Superconductors,* New York: Plenum Press, 1995.
38. C. Schmidt, Stability of superconductors in rapidly changing magnetic fields, *Cryogenics,* **30**: 501, 1990.
39. D. L. Walker et al., SMES conductor design, *IEEE Trans. Magn.,* **25**: 1596, 1989.
40. S. D. Peck, J. C. Zeigler, and C. A. Luongo, Tests on a 200 kA Cable-in-Conduit Conductor for SMES Application, *IEEE Trans. Appl. Supercond.,* **4**: 199, 1994.
41. L. Bottura, Stability, protection and ac loss of cable-in-conduit conductors—A designer's approach, *Fus. Eng. Des.,* **20**: 351–362, 1993.
42. E. Tada et al., Downstream effect on stability in cable-in-conduit superconductor, *Cryogenics,* **29**: 830, 1989.
43. N. Koizumi et al., Experimental results on instability caused by non-uniform current distribution in the 30 kA NbTi Demo Poloidal Coil (DPC) conductor, *Cryogenics,* **34**: 155, 1994.
44. N. Koizumi et al., Current imbalance due to induced circulation current in a large cable-in-conduit superconductor, *Cryogenics,* **36**: 409–418, 1996.
45. S. Jeong et al., Ramp-rate limitation experiments using a hybrid superconducting cable, *Cryogenics,* **36**: 623–629, 1996.
46. P. J. Giarratano and W. G. Steward, Transient forced convection heat transfer to helium during a step in heat flux, *Trans. ASME,* **105**: 350–357, 1983.
47. W. B. Bloem, Transient heat transfer to a forced flow of supercritical helium at 4.2 K, *Cryogenics,* **26**: 300–308, 1986.
48. S. Van Sciver, *Helium Cryogenics,* New York: Plenum Press, 1979.
49. L. A. Yaskin et al., A correlation for heat transfer to superphysical (*sic*) helium in turbulent flow in small channels, *Cryogenics,* **17**: 549–552, 1977.
50. P. J. Giarratano, V. D. Arp, and R. V. Smith, Forced convection heat transfer to supercritical helium, *Cryogenics,* **11**: 385–393, 1971.

LUCA BOTTURA
CERN

CÉSAR LUONGO
Bechtel